The Walk-&-Roller: A Multimodal Robotic Vehicle Capable of Quasistatic Three-Legged Rolling Motion

Mahmood Karimi¹, Ky Woodard, Benjamin A. Sams and Thomas R. Bewley

Abstract—This paper presents a new quasi-static gait called end-over-end motion for a 3-legged robot, named the Walk-&-Roller (W&R). In this motion, walking is achieved through rotation of the main body of the robot in three gait phases. The rotational motion is performed by holding the robot on two of the legs and swinging the third over the body into a new forward position. The trajectory planning to achieve this gait is determined in such a way that the static tipover stability is guaranteed and no singularities are reached. Computer simulation and experiments have been executed to demonstrate the validity of this proposed gait method.

I. Introduction

WHENthe terrain is uneven or obstacles exist along the path, legged locomotion has clear advantages over rolling and track locomotion through its discontinuous contact with the ground as well as environmental adaptability. These advantages include improved mobility, traversing of large obstacles, energy efficiency, and stability enhancement [1],[2],[3].

Extensive research into the area of multi-legged robots has been done over the last few decades with the most common vehicles being bipeds, quadrupeds, hexapods [4],[5]. Among these, three limb robots have been investigated in various aspects of the design space and gaits for walking tasks.

Lyons and Pamnany in [6] developed a novel triped, called a rotopod. Through the use of a rotating arm, the robot is able to store up energy just like a flywheel. When one of the actuated legs is shortened, the opposite two legs lift off of the ground and the rotating arm causes the body to pivot around the shortened leg.

At the Florida Institute of Technology, work has been done to analyze a theoretical three-legged walking vehicle [7]. From a tripod stance, the robot swings one of its legs in between the other two. This swinging motion forces the robot to pivot over the two supporting legs and land on the swinging leg. Since the robot is constrained to moving along a triangular grid, straight-line motion can be achieved by repeating a three-step pattern.

Similar to the work done at the Florida Institute of Technology, researchers at Virginia Tech have developed a three-legged walking machine that uses the displacement of its center of mass to move efficiently [2]. After stabilizing itself in a tripod stance, the "STriDER" shifts its center of mass in the direction it intends to move. This causes the vehicle to become unstable and fall forward allowing the

The Authors are with the Coordinated Robotics Lab at University of California, San Diego, CA 92093 USA, ¹(e-mail: m7744k@yahoo.com).

trailing leg to swing under the two supporting legs to catch the body as it comes down. The repetition of this gait permits locomotion in a series of directions.

Another tripod-walking robot again uses a shifting of the center of mass to allow for motion, but in a much different way [1]. The vehicle has a balancing mass above the legs that rotates into a position over the supporting legs while the final leg moves into a new position. The balancing mass allows the vehicle to manipulate the position of its center of mass independent of the leg motion, which allows for lower degrees of freedom required for the legs.

The generation of a gait can be subdivided into two main categories, static and dynamic gaits. For rapid locomotion, the dynamic gait must be applied to compensate for inertial forces caused by quick movement. On the other hand, a static gait, which is considered in this paper, should be used when the movements are slow and more importance is placed on stability of the center of mass (COM) within the supporting polygon [8].

The W&R, built in the Coordinated Robotics Lab at UCSD, is a 3-legged robot which is mechanically similar to the LIBRA developed at MIT [9]. Unlike the LIBRA, the joint motors of the W&R have been placed in the main body to make it possible for future developments in the 3D case. Due to this distinction, the legs are significantly lighter and improve the versatility of the W&R to many different types of locomotion as well as obstacle avoidance [10]. This paper presents a new quasi-static gait called end-over-end motion for the W&R. Firstly, the W&R and characterization of the new gait are described. Then, velocity kinematics for the purposes of modeling is derived. Next, the time-trajectories are planned for the gaits and the control procedure is explained.

II. THE WALK & ROLLER

The W&R robot consists of a central triangular body frame called the hub, which is attached to the three legs as depicted in Fig. 1(a). Each leg is made up of two links and two actuated revolute joints. The robot thus has a total of 9 degrees of freedom. The Walk-&-Roller was designed to be symmetric in order to remove any directional bias. The final vehicle will be composed of two identical halves capable of acting in unison or independently (see Fig. 1(b)). This allows for the robot to follow both a straight and curved pathway as well as maneuver over obstacles.

This platform provides agility for a robot capable of rolling like a wheel with a varying radius, shuffling, climbing through vertical ducts and creeping at a very compact height.

III. PROBLEM DESCRIPTION

The Walk-&-Roller can operate in a series of different modes to achieve the desired translational motion, such as rolling and shuffling. Here, the main focus of this paper is a walking gait that is performed via rolling of the body. This end-over-end motion of the legs forces the entire system to roll and consequently produce translational motion. The rolling motion is performed by supporting the robot on two of the legs and rotating the third over the hub into a new forward position. In this motion, the center of mass can be repositioned further forward than in other conventional legged robots.

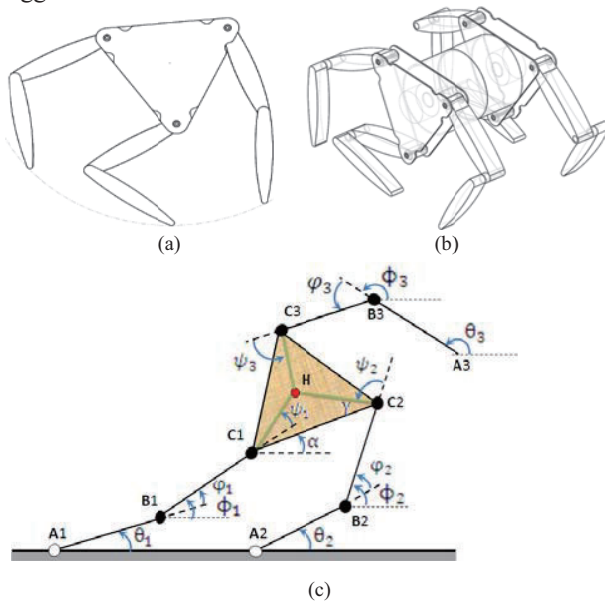


Figure 1: The Walk & Roller

In order to perform this motion, the following assumptions are made: 1- The robot moves with low velocity and acceleration so that the dynamic effects of the system can be ignored. 2- The robot's footpads contact a terrain with known geometry, and each contact provides enough friction to prevent the foot from slipping.

These assumptions allow for the system to be simplified as a serial-parallel manipulator. Since the W&R has three independently actuated limbs, three separate sets of kinematic equations can be derived depending on which leg is performing the swinging motion.

IV. CHARACTERIZATION OF THE W&R GAIT

Figure 1(c) shows a schematic of the leg configuration in the vertical plane with its design parameters. A1 and A2 represent the supporting feet, which are in contact with the ground, and A3 represents the swinging foot.

One cycle of the end-over-end gait can be broken down into the following three steps

- (I) Translation of the hub to improve the tipover stability of the robot
- (II) Translation and rotation of the hub while simultaneously swinging the 3rd leg in joint space

(III) Point to point motion of the tip of the 3rd leg in Cartesian space

In phase (I), all three legs are in contact with the ground so that the hub can translate forward horizontally with appropriate rotation (fig. 2). This motion brings the COM above the two forward legs, and as a result improves the robot's tipover stability for the end-over-end motion. In this phase, the tip of the prospective swinging leg follows the hub motion to prevent singularities from occurring.

In phase (II), the joint angles of the swinging leg as well as the COM position and orientation of the hub are forced to follow planned trajectories (fig. 3). This motion brings the hub into its desired position but since joint space has no concept of ground, the third leg reaches a final position slightly above the ground. Due to the rotational limitations of the leg joints, it is necessary to perform trajectory planning in joint space for large displacements of the swinging leg.

In phase (III), the swinging leg is driven to a desired position on the ground by point to point position control of the tip while the hub remains stationary (fig. 4). Therefore, the trajectory planning has to be derived in task space for both the hub and the swinging leg.

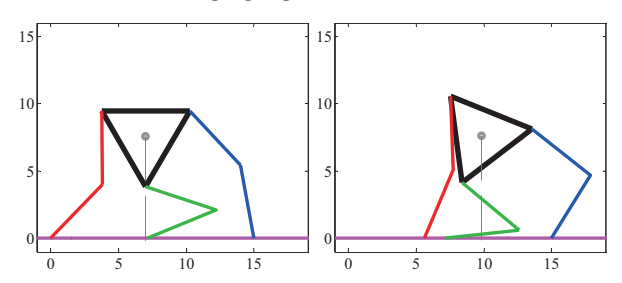
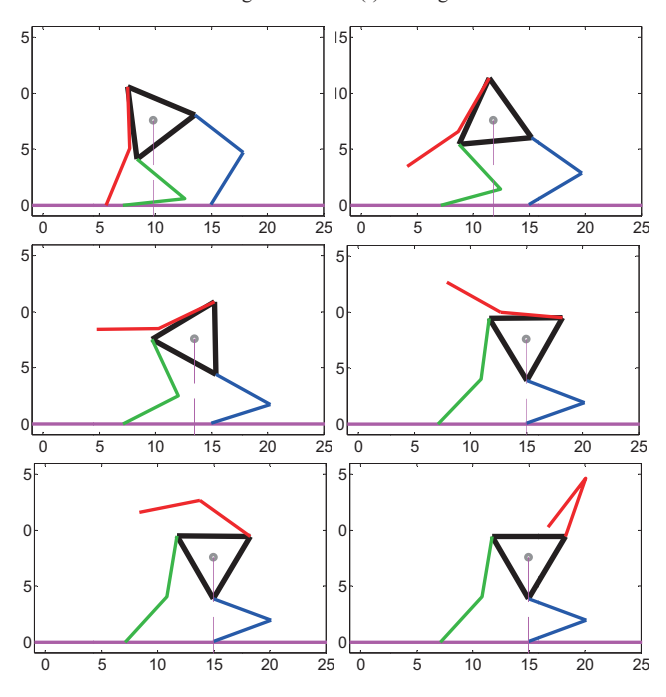


Figure 2: Phase (I) of the gait



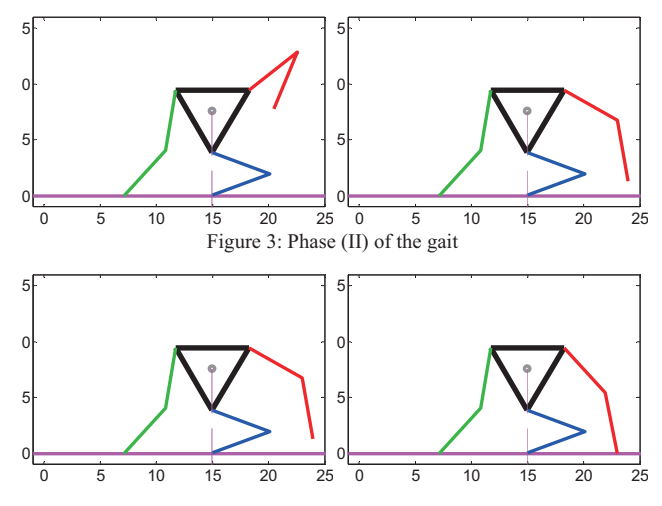


Figure 4: Phase (III) of the gait

V. VELOCITY KINEMATICS

For planning the gait and computing control velocity inputs, the relationship between task space and joint space must be determined. The joint variables are taken from the rotation of the six leg segments. The task space for phases (I) through (III) is represented by the set of Cartesian variables defined by the position of the center of mass of the hub, the orientation of the hub, and also the position vector of the tip of the swinging leg for phase (I) and (III) and the joint angles of the swinging leg for phase (II).

4.1. Absolute Angles

Considering θ_i and ϕ_i to be the absolute angles of the *i*-th leg and α to be the absolute rotation of the hub, the goal is to map the output velocity vector to the absolute angles of the legs. To this end, the swinging leg is always assumed to be the 3rd leg, and the left and right supporting legs are considered to be the 1st and 2nd respectively. The linear velocity vector of point H, h can be obtained in two different forms, depending on which leg is traversed, namely,

 $\dot{\mathbf{h}} = \dot{\theta}_{i} \mathbf{E} (\mathbf{b}_{i} - \mathbf{a}_{i}) + \dot{\phi}_{i} \mathbf{E} (\mathbf{c}_{i} - \mathbf{b}_{i}) + \dot{\alpha} \mathbf{E} (\mathbf{h} - \mathbf{c}_{i})$ in which i=1,2 and \mathbf{a}_i , \mathbf{b}_i , and \mathbf{c}_i are linear velocity vectors of the points Ai, Bi and Ci, respectively. The matrix E is defined as

$$\mathbf{E} = \begin{bmatrix} 0 & -1 \\ 1 & 0 \end{bmatrix} \tag{2}$$

Equation (1) can now be written in vector form as

Equation (1) can now be written in vector form as
$$\begin{bmatrix}
\mathbf{I} & -\mathbf{E}(\mathbf{h} - \mathbf{c}_1) \\
\mathbf{I} & -\mathbf{E}(\mathbf{h} - \mathbf{c}_2)
\end{bmatrix} \begin{bmatrix} \dot{\mathbf{h}} \\ \dot{\alpha} \end{bmatrix} = \\
\begin{bmatrix} \mathbf{E}(\mathbf{b}_1 - \mathbf{a}_1) & \mathbf{E}(\mathbf{c}_1 - \mathbf{b}_1) & \mathbf{0} & \mathbf{0} \\ \mathbf{0} & \mathbf{0} & \mathbf{E}(\mathbf{b}_2 - \mathbf{a}_2) & \mathbf{E}(\mathbf{c}_2 - \mathbf{b}_2) \end{bmatrix} \begin{bmatrix} \dot{\mathbf{q}}_{abs \ 1} \\ \dot{\mathbf{q}}_{abs \ 2} \end{bmatrix} \tag{3}$$
with $\dot{\mathbf{q}}_{abb} = \mathbf{0}$, $\dot{\mathbf{q}}_{abb} = \mathbf{0}$, $\dot{\mathbf{q}}_{abb} = \mathbf{0}$, $\dot{\mathbf{q}}_{abb} = \mathbf{0}$.

with $\dot{\mathbf{q}}_{abs i} = \begin{bmatrix} \dot{\theta}_i \\ \dot{\phi}_i \end{bmatrix}$ being the vector of absolute joint rates of

the *i*-th leg and $\mathbf{0}$ is a 2×1 zero matrix.

For phases (I) and (III), the velocity of point A_3 (\dot{a}_3) can be obtained using the velocity of point C3, which is derived in two different ways, namely,

$$\dot{\mathbf{a}}_3 + \dot{\theta}_3 \mathbf{E}(\mathbf{b}_3 - \mathbf{a}_3) + \dot{\phi}_3 \mathbf{E}(\mathbf{c}_3 - \mathbf{b}_3) = \dot{\alpha} \mathbf{E}(\mathbf{c}_3 - \mathbf{h}) + \dot{\mathbf{h}}$$
 (4)

Equation (4) can now be rewritten in vector form as

$$\begin{bmatrix} \mathbf{I} & \mathbf{E}(\mathbf{c}_3 - \mathbf{h}) & -\mathbf{I} \end{bmatrix} \begin{bmatrix} \dot{\mathbf{h}} \\ \dot{a} \\ \dot{a}_3 \end{bmatrix} = \begin{bmatrix} \mathbf{E}(\mathbf{b}_3 - \mathbf{a}_3) & \mathbf{E}(\mathbf{c}_3 - \mathbf{b}_3) \end{bmatrix} \dot{\mathbf{q}}_{abs \ 3} \quad (5)$$

4.2. Relative Angles

Considering that φ_i and ψ_i are the relative angles of *i*-th leg depicted in Fig. 1(c), the relationship between the rates of the absolute and relative angles can be represented as

$$\dot{\mathbf{q}}_{abs\,i} = \mathbf{F}\dot{\mathbf{q}}_{rel\,i} + \begin{bmatrix} 1\\1 \end{bmatrix} \dot{\alpha} \quad i=1,2,3 \tag{6}$$

in which $\dot{\bm{q}}_{rel~i} = \begin{bmatrix} \dot{\phi}_i \\ \dot{\psi}_i \end{bmatrix}$ is the vector of relative actuated joint

rates and the matrix \mathbf{F} is defined as

$$\mathbf{F} = \begin{bmatrix} -1 & -1 \\ 0 & -1 \end{bmatrix} \tag{7}$$

By substituting $\begin{bmatrix} \dot{\mathbf{q}}_{abs 1} \\ \dot{\mathbf{q}}_{abs 2} \end{bmatrix}$, constructed from Eq. (6), into Eq.

(3) and performing some manipulation, the following is

$$\begin{bmatrix} I & -E(b_1-a_1) - E(c_1-b_1) - E(h-c_1) \\ I & -E(b_2-a_2) - E(c_2-b_2) - E(h-c_2) \end{bmatrix} \begin{bmatrix} \dot{h} \\ \dot{\alpha} \end{bmatrix} = \\ \begin{bmatrix} E[(b_1-a_1) & E(c_1-b_1)]F & 0 & 0 \\ 0 & 0 & E[(b_2-a_2) & E(c_2-b_2)]F \end{bmatrix} \begin{bmatrix} \dot{q}_{\rm rel~1} \\ \dot{q}_{\rm rel~2} \end{bmatrix}$$
 (8) Also for phases (I) and (III), the subsequent relation can be

obtained through the substitution of $\dot{\mathbf{q}}_{abs\,3}$ from Eq. (6) into

$$\begin{bmatrix} \mathbf{I} & \mathbf{E}(\mathbf{a}_3 - \mathbf{b}_3) + \mathbf{E}(\mathbf{b}_3 - \mathbf{c}_3) + \mathbf{E}(\mathbf{c}_3 - \mathbf{h}) & -\mathbf{I} \end{bmatrix} \begin{bmatrix} \dot{\mathbf{h}} \\ \dot{\alpha} \\ \dot{\mathbf{a}}_3 \end{bmatrix} = \begin{bmatrix} \mathbf{E}(\mathbf{b}_3 - \mathbf{a}_3) & \mathbf{E}(\mathbf{c}_3 - \mathbf{b}_3) \end{bmatrix} \mathbf{F} \dot{\mathbf{q}}_{\text{rel } 3}$$
(9)

VI. TRAJECTORY PLANNING

In this section, the trajectory planning is performed for all phases of the gait using point to point motion. The polynomial functions in terms of time are used to define trajectories for the hub position/orientation and joint angles and tip of the swinging leg. The third-order (cubic) polynomials are the lowest order polynomials for which it is possible to specify both position and speed. Due to obstacle avoidance and joint limitation, redundancy in the polynomial to design the desired trajectory is needed.

$$p(t) = k_0 + k_1 t + k_2 t^2 + k_3 t^3 + k_4 t^4$$
 (10)

It is necessary to determine the coefficients corresponding to each cubic polynomial. By considering (10), taking its first derivative with respect to time at both the start and the end, and also taking an additional position equation at the desired t_{i*} into consideration, five equations can be derived. Since the position and its speed are known at the beginning and the end and the redundant position is determined based on the constraint, the system of five equations and five unknowns, $(k_0, k_1, k_2, k_3, k_4)$, can be solved,

$$\begin{bmatrix} 1 & t_{i} & t_{i}^{2} & t_{i}^{3} & t_{i}^{4} \\ 0 & 1 & 2t_{i} & 3t_{i}^{2} & 4t_{i}^{3} \\ 1 & t_{i*} & t_{i*}^{2} & t_{i*}^{3} & t_{i*}^{4} \\ 1 & t_{i+1} & t_{i+1}^{2} & t_{i+1}^{3} & t_{i+1}^{4} \\ 0 & 1 & 2t_{i+1} & 3t_{i+1}^{2} & 4t_{i+1}^{3} \end{bmatrix} \begin{bmatrix} k_{0} \\ k_{1} \\ k_{2} \\ k_{3} \\ k_{4} \end{bmatrix} = \begin{bmatrix} p(t_{i}) \\ \dot{p}(t_{i}) \\ p(t_{i*}) \\ p(t_{i*}) \\ \dot{p}(t_{i+1}) \\ \dot{p}(t_{i+1}) \end{bmatrix}, 1 \le i \le 3$$
 (11)

in which t_i and t_{i+1} are the initial and final time of i-th phase of the gait and $t_i < t_{i*} < t_{i+1}$. The coefficients can be determined by considering the following conditions

 $p(t_i) = p_i, \dot{p}(t_i) = 0, p(t_{i+1}) = p_{i+1}, \dot{p}(t_{i+1}) = 0, p(t_{i*}) = p_{i*}$ wherep_i,p_{i+1}and p_{i*}are the desired initial, final and intermediate value of each control variable in the i-th phase. Here, it is considered in our test that the environment is free of obstacles and the surface is flat. Therefore, the desired horizontal and vertical center of mass positions of the hub (h_x, h_y) at the beginning and end of each phase of the gait can be written as:

$$(h_{x}, h_{y}, h_{\alpha}) = \begin{cases} (h_{xa}, h_{ya}, h_{\alpha a}) & t = t_{1} \\ (h_{xb}, h_{ya}, h_{\alpha b}) & t = t_{2} \\ (h_{xc}, h_{ya}, h_{\alpha c}) & t = t_{3} \end{cases} \begin{cases} Phase (II) \\ Phase (III) \\ Phase (III) \end{cases}$$

and II respectively due to the tipover stability improvement and translational motion. Also, $h_{\alpha b} - h_{\alpha a}$ is the increment of h_{α} in phase I and helps in the translational motion to improve tipover stability. $h_{\alpha c} - h_{\alpha b}$ is the increment of h_{α} in phase II to make the main translation possible. Due to the lack of obstacles and flat surface, $h_v = h_{va}$ in all phases.

The desired horizontal and vertical tip positions of the swinging leg (a_{3x}, a_{3y}) at the beginning and end of phases (I) and (III) are represented by:

$$(a_{3x}, a_{3y}) = \begin{cases} (a_{3xa}, a_{3ya}) & t = t_1 \\ (a_{3xb}, a_{3yb}) & t = t_2 \end{cases} \quad \text{Phase (I)}$$

$$(a_{3xc}, a_{3ya}) & t = t_3 \\ (a_{3xd}, a_{3ya}) & t = t_4 \end{cases} \quad \text{Phase (III)}$$

At the end of phase I, $a_{3y} = a_{3yb}$ is theoretically considered a bit larger than a_{3ya} in order to decrease friction force on the tip of the prospective swinging leg although a_{3yb} is equal to a_{3va} in the test. If the origin of the world coordinate is placed on the ground, $a_{3xa} = 0$. The desired initial and final values for the joint angles of the swinging leg in phase II are given as

$$(\theta_3, \phi_3) = \begin{cases} (\theta_{3a}, \phi_{3a}) & t = t_2 \\ (\theta_{3b}, \phi_{3b}) & t = t_3 \end{cases}$$
 Phase (II) (15)
$$\theta_{3b} \text{ and } \phi_{3b} \text{ are chosen so that the final location of the tip}$$

of the swinging leg is slightly above the ground.

VII. TIPOVER STABILITY MEASURE

In the first phase of the gait, improving tipover stability by hub translation and rotation is necessary to prevent the subsequent phase from reaching instability. Hence, the desired position/orientation of the center of mass of the hub as well as the tip of the prospective swinging leg must be appropriately determined in such a way that stability improves and none of the legs are forced to overextend or driven theoretically underground. To this end, the middle and right legs are considered to be the support legs, and the left one is designated as the swinging leg when the robot is traveling towards the right hand side, and vice versa when the robot motion is toward the left.

In our work, the force-angle tipover stability measure is utilized in a manner similar to that proposed in [11],[12].

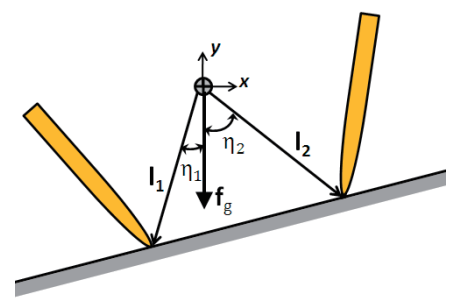


Figure 5: Stability definition diagram

Let l_i represent the instantaneous location of the i-th, $i=\{1,2\}$, ground contact point from the center of mass of the entire system and \mathbf{f}_g the gravitational force vector of the entire system (fig. 5). The stability angles can be computed for each tipover axis as the angle between the gravitational force vector \mathbf{f}_{g} and the position vector \mathbf{l}_{i}

$$\eta_{i} = \sigma_{i} \cos^{-1} (\hat{\mathbf{f}}_{g} \cdot \hat{\mathbf{i}}_{i}) \quad i = 1,2$$
(16)

with
$$\sigma_{i} = \begin{cases} +1 & (\hat{\mathbf{l}}_{i} \times \hat{\mathbf{f}}_{g}) \cdot \hat{\mathbf{p}}_{i} \text{ with } \hat{\mathbf{p}}_{1} = [0; 0; -1], \; \hat{\mathbf{p}}_{2} = [0; 0; 1] \end{cases}$$

$$\Delta \mathbf{r}_{i} = \begin{cases} +1 & (\hat{\mathbf{l}}_{i} \times \hat{\mathbf{f}}_{g}) \cdot \hat{\mathbf{p}}_{i} \text{ with } \hat{\mathbf{p}}_{1} = [0; 0; -1], \; \hat{\mathbf{p}}_{2} = [0; 0; 1] \end{cases}$$

$$\Delta \mathbf{r}_{i} = \begin{cases} +1 & (\hat{\mathbf{l}}_{i} \times \hat{\mathbf{f}}_{g}) \cdot \hat{\mathbf{p}}_{i} \text{ with } \hat{\mathbf{p}}_{1} = [0; 0; -1], \; \hat{\mathbf{p}}_{2} = [0; 0; 1] \end{cases}$$

And $\hat{*}=*/||*||$. The overall planar W&R stability angle is defined as the minimum of the two stability angles:

$$\beta = \min(\eta_i) \tag{18}$$

Tipover instability can occur when β < 0. Measurements of the leg contact forces or joint torques are not required, since kinematics-based stability analysis is being implemented. Keeping this in mind, the planning attempts to preserve a relatively large value for β .

VIII. W&R CONTROL

The W&R can be controlled through inverse velocity kinematics, which requires closed-loop control of all the actuators simultaneously using

$$\begin{bmatrix} \dot{\mathbf{h}} \\ \dot{\alpha} \\ \dot{\mathbf{a}}_{3} \end{bmatrix} = \begin{bmatrix} \dot{\mathbf{h}}_{\text{des}} \\ \dot{\alpha}_{\text{des}} \\ \dot{\mathbf{a}}_{3 \text{ des}} \end{bmatrix} + \lambda \begin{bmatrix} \mathbf{e}_{\text{h}} \\ \mathbf{e}_{\alpha} \\ \mathbf{e}_{\text{a}} \end{bmatrix}$$
(19)

$$\begin{bmatrix} \mathbf{e}_{\mathbf{h}} \\ \mathbf{e}_{\alpha} \\ \mathbf{e}_{\mathbf{a}} \end{bmatrix} = \begin{bmatrix} \mathbf{h}_{\text{des}} \\ \alpha_{\text{des}} \\ \mathbf{a}_{3,\text{des}} \end{bmatrix} - \begin{bmatrix} \mathbf{h} \\ \alpha \\ \mathbf{a}_{3} \end{bmatrix}$$
 (20)

and λ is a 6×6 diagonal gain matrix. The actuated joint variables, obtained by Eqs (8) and (9), are considered as the desired trajectories for the real world implementation. The physical joints then track these positions through the use of close-loop control.

The control of the motors is performed through an Arduino prototyping board and a set of Sabertooth 2×5 dual motor drivers. Feedback from the actual rotation is taken from the potentiometers attached to the joints. Due to the computational power of the control algorithm, the algorithm is performed on an external laptop in MATLAB and then commands are transmitted to the Arduino via a tether.

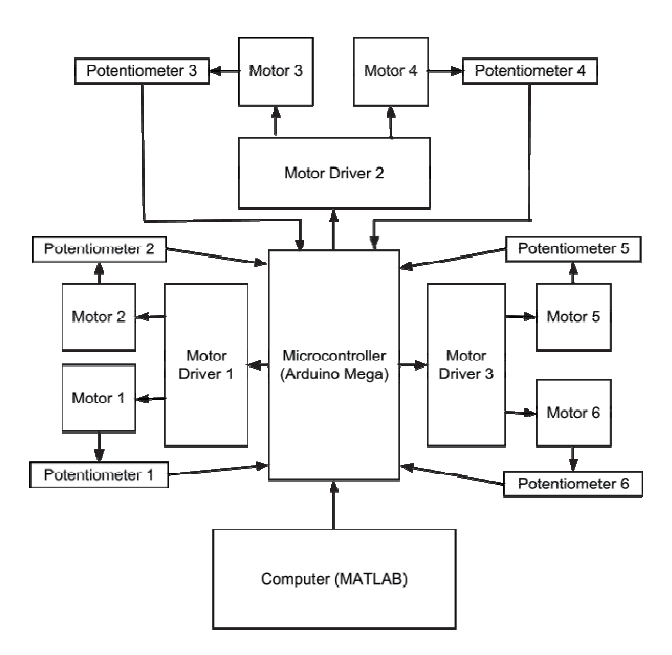


Figure 6: Electronic Diagram of the Walk-&-Roller Robot

The Arduino runs the Arduino IO package to allow MATLAB to directly access its pins. A diagram of this electronic setup is shown in Fig. 6.

IX. OBTAINED RESULTS

A prototype of the Walk-&-Roller robot has been built for the purposes of physical tests on the performance of the previously explained control system. The prototype was built out of aluminum plate cutouts to construct the overall hub and leg joints. The benefits of the aluminum frame include quick assembly along with added durability. Actuation of the joints is controlled by a set of six motors located centrally in the main body. The motor torque is transmitted to the individual joints through a series of timing belts, which are reinforced with Kevlar thread to improve the strength and limit the amount of relaxation over time. The following figure is the test of the leg motion while attempting to track the gait path:

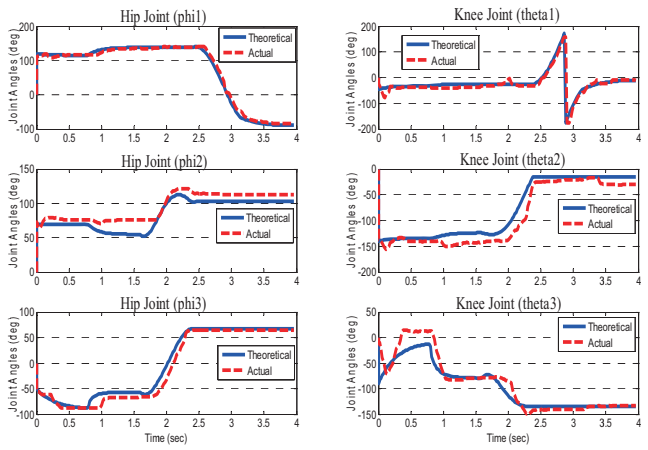
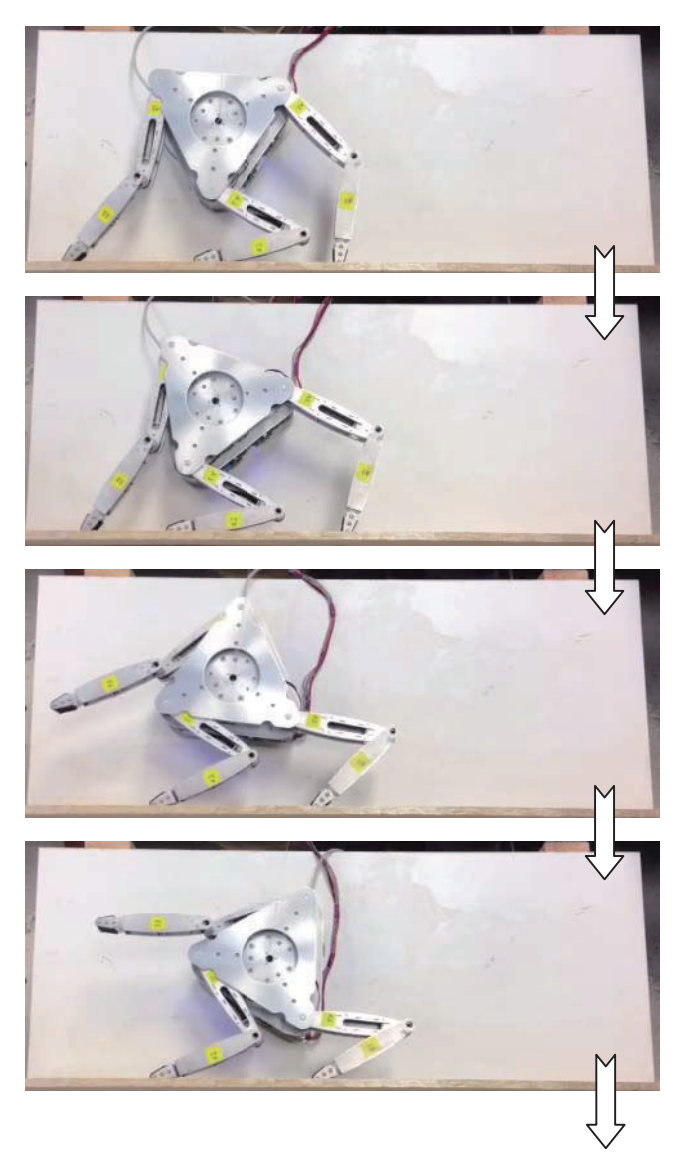


Figure 7: Simulation and experimental results

This test was performed while the robot was on a platform angled 46.8 degrees from vertical to reduce the gravitational force felt by the legs. With the current motors in use on the W&R, the robot must be tested at an angle instead of completely vertical. This reduces the force required for the robot to lift itself. The three plots in the left hand column of Figure 7 demonstrate the motion of the leg segments closest to the central hub. Despite minor offset due to the inaccuracy of the potentiometers, these segments tracked the theoretical values well. On the other hand, the outer legs were unable to efficiently track the theoretical leg positions. The reasons for this inaccuracy are mechanical losses in the timing belt gears due to insufficient machining tolerances.

The snapshot of the W&R performing the end-over-end motion is shown in the figure 8.



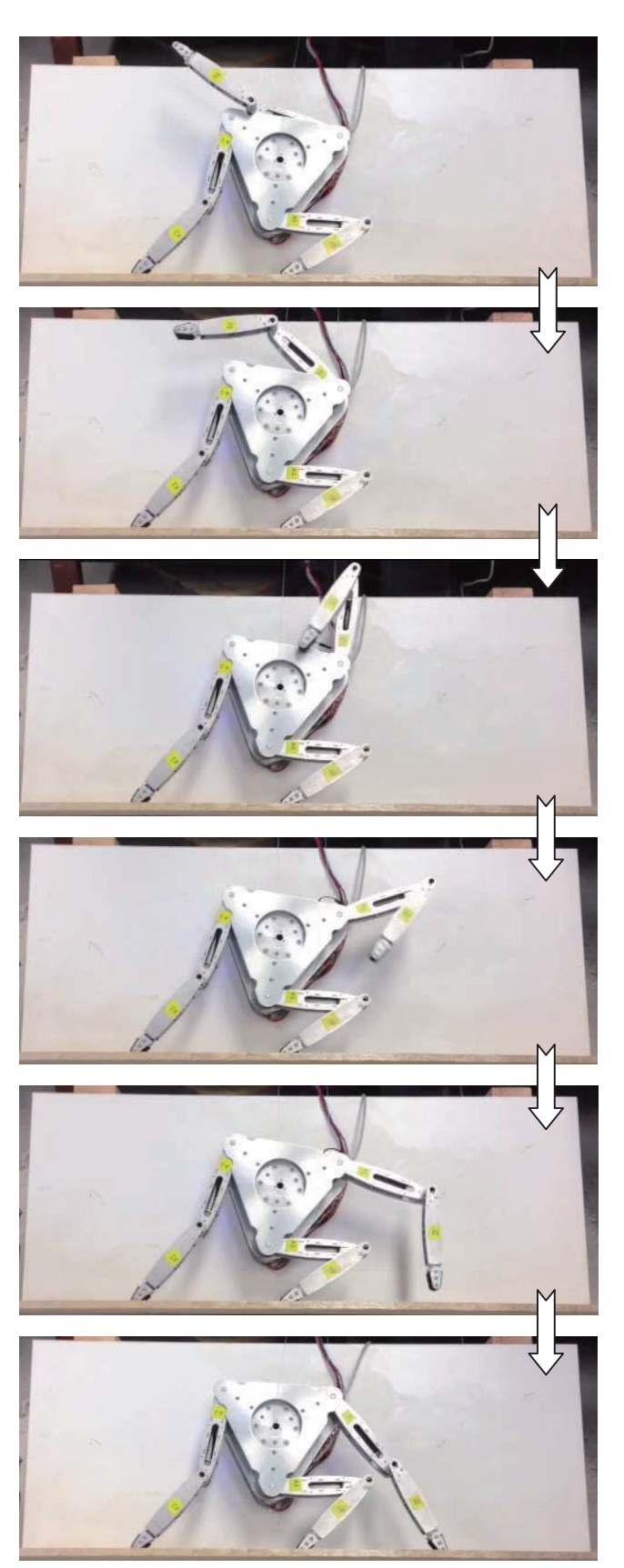


Figure 8: Snapshot

X. CONCLUSION

A new quasi-static gait called end-over-end motion for the W&R was presented in this paper. The walking was achieved in this motion through rotation of the main body of the robot and swinging a leg over the body when the other two legs hold the robot. A few assumptions were made to simplify the system to a serial-parallel manipulator. The performed simulation and experiments demonstrated the validity of this proposed gait method despite backlash in the joints.

REFERENCES

- C. Liang, H. Gu, M. Ceccarelli, and G. Carbone, "Design and operation of a tripod walking robot via dynamics simulation" Robotica, volume 29, pp. 733–743, 2011.
- [2] J. Heaston, D. Hong, I. Morazzani, P. Ren, and G. Goldman "STriDER: Self-Excited Tripedal Dynamic Experimental Robot" IEEE International Conference Robotics and Automation, Roma, Italy.2007
- [3] S. Ma, T. Tomiyama, and H. Wada, "Omnidirectional Static Walking of a Quadruped Robot" *IEEE TransactionsofRobotics*, Vol 21, No. 2, pp. 152-161,2005.
- [4] G. Carbone and M. Ceccarelli, "Legged Robotic Systems," Cutting Edge Robotics ARS Scientific Book, Wien, pp. 553–576, 2005.
- [5] Q. Wu, C. Liu, J. Zhang and Q. Chen "Survey of locomotion control of legged robots inspired by biological concept" *Science in China Series F: Information Sciences*, Volume 52, Number 10, pp. 1715-1729, 2009.
- [6] D. Lyons and K. Pamnany "Rotational legged locomotion" IEEE International Conference on Advanced Robotics, Seattle WA, July 2005.
- [7] D. Kamerling, and P. Larochelle, "Proposed Design of a Triped Robot" Proceedings of the 2007 Florida Conference on Recent Advances in Robotics, Tampa, Florida, 2007.
- [8] D. Son and et. al., "Gait planning based on kinematics for a quadruped gecko model with redundancy" Robotics and Autonomous Systems, 58(5), pp. 64-656, 2010.
- [9] D.M. Bevly, S. Farritor and S. Dubowsky "Action Module Planning and its Application to an Experimental Climbing Robot" IEEE International Conference on Robotics Automation, San Francisco, CA, 2000.
- [10] Benjamin A. Sams "Design and Analysis of an Articulated Spoke Multi-Modal Robot and Design and Implementation of Object Manipulation Features" M.Sc. Thesis, University of California, San Diego.
- [11] Papadopoulos, E. and Rey, D., "The Force-Angle Measure of Tipover Stability Margin for Mobile Manipulators," Vehicle System Dynamics, Vol. 33, No 1, 2000.
- [12] Iagnemma, K., Rzepniewski, A., Dubowsky, S., and Schenker, P., "Control of Robotic Vehicles with Actively Articulated Suspensions in Rough Terrain," Autonomous Robots, Volume 14, Number 1, pp. 5-16, 2003